# Nanoparticle detection using fano-resonance photonic crystal on optical fiber-tip

Daquan Yang, Wei Yuan, Yuefeng Ji

Daquan Yang, Wei Yuan, Yuefeng Ji, "Nanoparticle detection using fano-resonance photonic crystal on optical fiber-tip," Proc. SPIE 10158, Optical Communication, Optical Fiber Sensors, and Optical Memories for Big Data Storage, 101581I (25 October 2016); doi: 10.1117/12.2247427

Event: International Symposium on Optoelectronic Technology and Application 2016, 2016, Beijing, China

# Nanoparticle detection using Fano-resonance photonic crystal on optical fiber-tip

**Daquan Yang[1], Wei Yuan[1] and Yuefeng Ji[1, *]**

*[1]State Key Laboratory of Information Photonics and Optical Communications (IPOC), School of Information and Communication Engineering, Beijing University of Posts and Telecommunications (BUPT), Beijing 100876, China.*

## Abstract

Recently, Fano-resonance photonic crystals (PhC) have been employed within a wide variety of nanophotonic structures for different applications, including imaging, filtering, switching, sensing, and so on. In this paper, we propose a convenient and compact fiber-optic sensor based on optical fiber-tips integrated with Fano-resonance pillar-array PhC. The quality factor $1.04\times10^4$ and refractive index sensitivity of 226 nm per refractive index unit (RIU) have been demonstrated. In addition, the proposed Fiber-PhC integrated senor structure can be used for nanoparticle detection by checking the reflection spectrum shift with a narrow line-width. Using this method, we demonstrate that the detection of polystyrene nanoparticles with dimensions down to 50 nm in radius can be achieved. Thus, we believe that the design and results presented here are promising and enable the implementation of simple but functional fiber-optic sensors and devices.

**Key words:** Optical fiber-tip sensor, Photonic crystal, High-Q resonance, Nanoparticle detection.

## 1. Introduction

Optical fibers can be used as sensors to measure strain, temperature, pressure and other physical quantities by modifying a fiber so that the physical quantity to be measured modulates the intensity, phase, polarization, wavelength or transit time of light in the fiber. Recently, a wide variety of fiber optic sensors based on fiber Bragg gratings (FBG) [1-3], surface plasmon resonance (SPR) [4-6], Mach-Zehnder interference [7-9], and Fabry-Perot interference [10-12] have been investigated and demonstrated. In the last few years, significant progress has been made in semiconductor photonic crystal (PhC) due to their extensive applications. Their use as sensors generates significant interest because of their ability to confine light to ultra-compact mode volumes and their high sensitivity to a very small variation in refractive index of the surrounding, making it easy to create high-density integrated micro sensors arrays [13-17].

* jyf@bupt.edu.cn

Optical Communication, Optical Fiber Sensors, and Optical Memories for Big Data Storage,
edited by Yanbiao Liao and Xiaodi Tan, Proc. of SPIE Vol. 10158, 101581I © 2016 SPIE
CCC code: 0277-786X/16/$18 · doi: 10.1117/12.2247427

With the development of Fano-resonance sensors, such sensors based on optical fibers became more popular due to their unique advantages over electronic systems, such as small size, high sensitivity, immunity to electromagnetic interference, lower cost, chemical and mechanical robustness and distributed sensing capabilities. Recently, some research groups have developed various methods to functionalized optical fiber tips integrated with semiconductor PhC by using several different transfer processes, which aims at coupling between PhC chips and fibers conveniently, simply and efficiently [18-20]. In this paper, a novel Fiber-PhC sensor based on optical fiber tips integrated with Fano resonance pillar-array photonic crystal is proposed and demonstrated. By using three-dimensional finite difference time domain (3D-FDTD) method, the calculated Q-factor is ultra-high which can reach the fourth power of 10 in orders of magnitude. Comparing with the Q-factors of those fiber-optic photonic crystal (Fiber-PhC) sensors [18-20], which are low around ~1000, this parameter is one order of magnitude improved. Also, an optical fiber tip integrated with Fano resonance pillar-array photonic crystal refractive index sensor of 226 nm per refractive index unit sensitivity has been demonstrated.

Here, we also study the effect of the introduction of a nanoparticle into the Fano-resonance pillar-array photonic crystal by simulations. We analyze the transmission spectra of the Fiber-PhC sensor when no particle is placed and when a nanoparticle is placed centrally on the top of the designed Si-PhC pillar array. Using this approach, we demonstrate that the detection of polystyrene nanoparticles with dimensions down to 50 nm in radius can be achieved.

## 2. Fiber-PhC sensor design and characterization

Fano resonances (also called guided resonance), known from atomic physics, have been employed for a wide variety of nano photonic structures, e.g. PhC [21-23]. PhC slabs (PCSs) are one of the most promising artificial platforms with in-plane periodic modulation of dielectric constant on a wavelength scale. The out of-the-plane optical mode coupling is feasible with the Fano or guided resonance effect, where these in-plane guided resonances above the light line are also strongly coupled to out-of-the-plane radiation modes due to phase matching provided by the periodic lattice structure. Therefore, the guided resonances can provide an efficient way to channel light from within the slab to the external environment, and vice versa [24]. The property of guided resonances holds promise for several potential applications, such as filters, modulators and sensors. Thus, based on the Fano resonance in pillars-array PhC, we propose a novel fiber-optic PhC refractive index sensor consisted of an optical fiber tip integrated with pillar-array PhC. Fig. 1 shows a schematic of the optical setup for objects measurements with different refractive index. Area marked by blue dashed box shows the Fiber-PhC sensor. As we can see from the figure, light from light source (a tunable laser) is coupled into the Fiber-PhC sensor through a 3-ports optical circulator and reflected back into the fiber core where it can be subsequently detected by the optical detector. The optical fiber displayed we used is the standard optical communications fiber. The diameter of the fiber core is 8~10 μm, and the diameter of the fiber cladding is 125 μm.

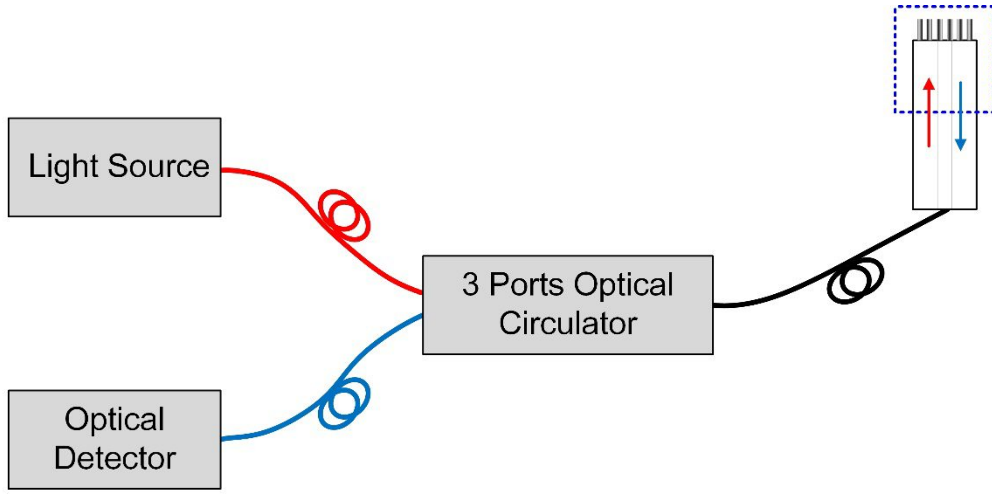


Fig. 1 (color online) Schematic of the optical setup for objects measurements with different refractive index, area marked by blue dashed box shows the Fiber-PhC sensor, we use 3 ports optical circulator to channel the light source, optical detector, and Fiber-PhC sensor.

Shown in Fig. 2 is the close-up image of the pillar array PhC. Area marked by red dashed box shows the schematic of a unit cell of the designed Si-PhC pillar array used in the simulation based on the 3D-FDTD technique, where key lattice parameters are denoted as *r*, *h* ,*a* and *t*, for bulk radius and height for pillar, lattice constant and slab thickness, respectively. Here, PhC structure is constructed by arranging a triangular lattice of silicon pillars (refractive index $n$ = 3.46). The bulk radius and heights of Si-PhC pillar (gray color in Fig. 2) are 174 nm and 1.12 µm, respectively. The periodicity (lattice constant) is $a$ = 870 nm.

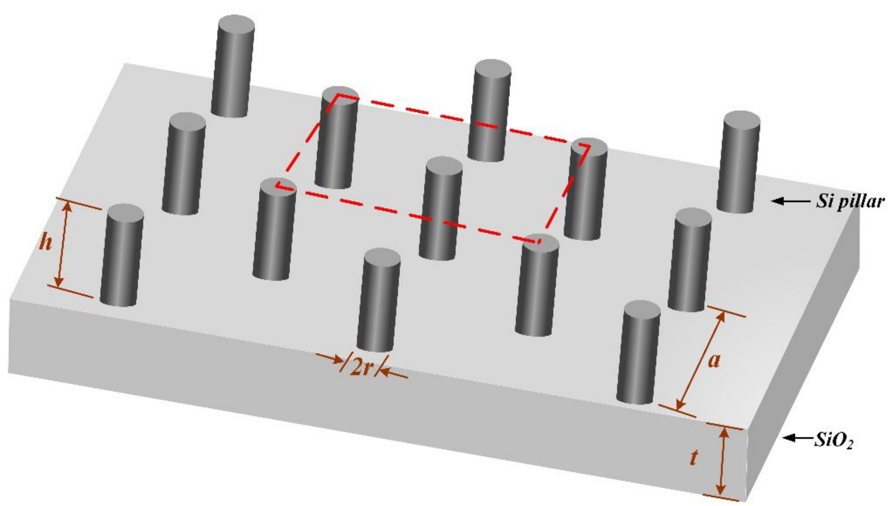


Fig. 2 (color online) The close-up image of the pillar array PhC. Area marked by red dashed box shows the schematic of a unit cell of the designed Si-PhC pillar array used in the simulation based on the 3D-FDTD technique. The key lattice parameters are denoted as *r*, *h*, *a* and *t*, for bulk radius and height for pillar, lattice constant and slab thickness, respectively.

Based on 3D-FDTD technique, the transmission spectrum at normal incidence of the proposed Fiber-PhC sensor in air

($n = 1.0$) is shown in Fig. 3. The insets display the fit to Lorentzian line shape for the Fano resonance at 1470.59 nm. As seen, the Lorentzian fit to the Fano resonance manifests a ultra-high Q-factor which can reach more than $1.04\times10^4$, and near 100% reflection is obtained. Thus, we can use the designed fiber-PhC sensor to sense the surrounding medium by analyzing the peak wavelength of the transmission spectrum with high sensitivity.

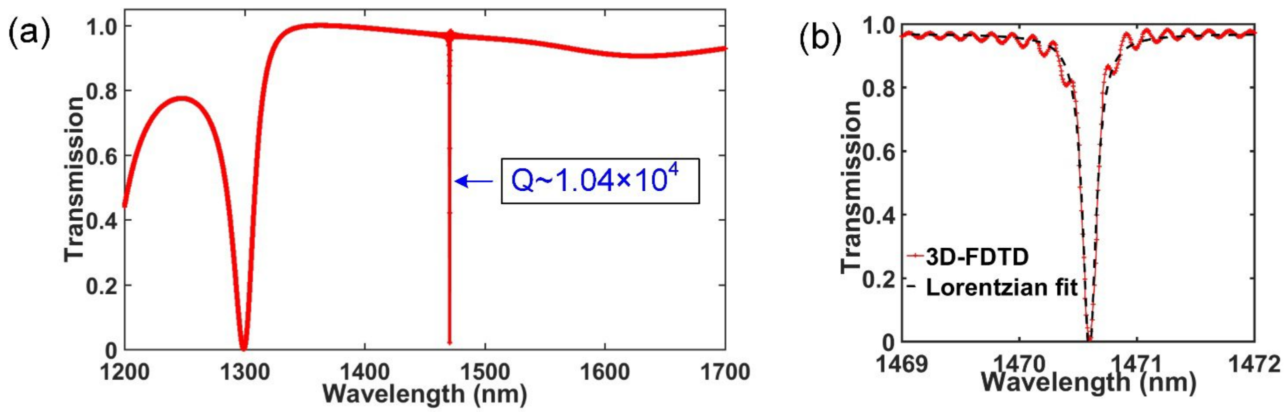


Fig. 3 (color online) (a) Transmission spectrum at normal incidence of the Fiber-PhC sensor in air. (b) Zoom-in the insets displays the fit to Lorentzian (Fano) line shape at 1470.59 nm. As seen, a Q-factor of $1.04\times10^4$, and near 100% reflection is obtained.

In order to investigate the refractive index sensitivity, the effect of varying refractive index of the dielectric environment surrounding the Fiber-PhC sensor region is operated by taking transmission spectra of the Fiber-PhC sensor in tested objects with different refractive index, RI = 1.0, 1.1, 1.2, and 1.3, respectively. Fig. 4 (a) shows the different transmission spectra of the Fiber PhC sensor. Fig. 4 (b) shows the relation between the refractive index of the surrounding medium and the corresponding resonant wavelength of the transmission peak. Slope of the curve represents the sensitivity of our design in unit of nm/RIU, where RIU is the refractive index unit. According to the resonant wavelengths shifts for the Fiber-PhC sensor immerged in different objects, the calculated refractive index sensitivity of device is about 226 nm/RIU with a linear fitting. We also can see from the Fig. 4 (b), the resonant wavelength moves toward longer wavelengths (red-shift) as the refractive index increases. Moreover, it is important to point out that the fabrication process of the proposed Fiber-PhC sensors is straight forward, low-cost and high throughout [16].

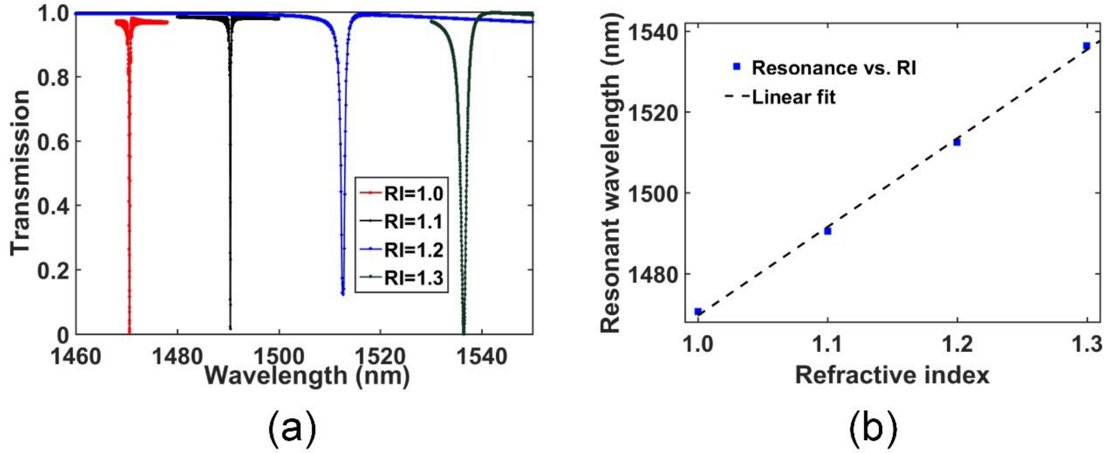


Fig. 4 (color online) (a) Composed transmission spectra of the Fiber-PhC sensor covered with objects with different refractive index. (b) Resonant wavelengths shifts toward longer wavelengths (red-shift) as the function of refractive index increases.

## 3. Analysis of nanoparticle detection

Other than sensing the surrounding medium by analyzing the peak wavelength of the reflection spectrum, the Fiber-PhC sensor based on optical fiber-tips integrated with Fano resonant pillar-array PhC can be used for nanoparticle detection. The detective objective is a polystyrene nanoparticle and the refractive index of the particle was taken to be that of polystyrene, $n = 1.59$ [25]. The radius of the particle was taken to be 50-100 nm, a typical size of polystyrene nanoparticle which is placed centrally on the top of the designed Si-PhC pillar array. Simulations with a nanoparticle of various size, radius = 0 nm, 50 nm, 75 nm, and 100 nm, respectively, show that as a function of the radius increase of a spherical nanoparticle located centrally on the top of the designed Si-PhC pillar array, the resonance wavelength of the transmission spectra shifts toward longer wavelength (red-shift). The color plot (indicated by black arrows in Fig. 4. (a)) makes clear the position of the nanoparticle and how its size is changed.

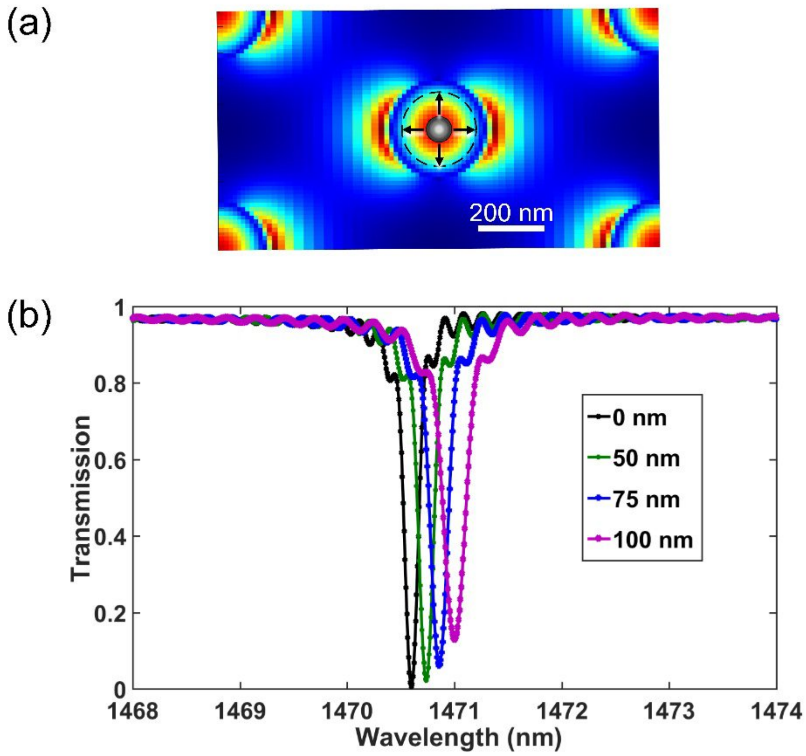


Fig. 5 (color online) (a) A spherical nanoparticle (100 nm diameter) sitting on top of the pillar array is centrally translated as shown in the color plot. (b) Transmission spectra of the Fiber-PhC sensor when no particle is placed and when a nanoparticle is placed centrally on the top of the designed Si-PhC pillar array. Polystyrene nanoparticles with dimensions down to 50 nm, 75 nm, 100 nm in radius can be achieved by checking the shift of the resonance wavelength with a narrow line-width.

## 4. Conclusions

In conclusion, we have proposed and demonstrated a convenient and compact Fiber-PhC sensor based on optical fiber-tips integrated with Fano resonant pillar-array PhC. From simulations, we find the quality factor of the proposed sensor can reach the fourth power of 10 ($1.04\times10^4$) in orders of magnitude. Refractive index sensor of 226 nm per refractive index unit (RIU) sensitivity has been demonstrated. Furthermore, we find that the proposed PhC fiber integrated sensor structure can be used for nanoparticle detection by checking the reflection spectrum shift with a narrow line-width. Using this approach, we demonstrate that the detection of polystyrene nanoparticles with dimensions down to 50 nm in radius can be achieved. The sensor has various potential applications, and can be further developed to improve its sensing capabilities for nanoparticle detection.

## 5. Acknowledgments

This work was supported in part by the NSFC under Grant No. 61501053, the Fund of the State Key Laboratory of Information Photonics and Optical Communications (BUPT: IPOC2015ZC03) and the Fundamental Research Funds for the Central Universities (BUPT), China.

## References


[1] X Shi, S Zheng, H Chi, X Jin, and X Zhang, "Refractive index sensor based on tilted fiber Bragg grating and stimulated Brillouin scattering," *Opt. Express* **20**, 10853-10858 (2012).

[2] U Sharath, C Shwetha, K Anandand S Asokan, "Radial arterial compliance measurement by fiber Bragg grating pulse recorder," *Nature: Journal of Human Hypertension* **28**, 736–742 (2014).

[3] W. Yuan, A. Stefani, and O. Bang, "Tunable Polymer Fiber Bragg Grating (FBG) Inscription: Fabrication of Dual-FBG Temperature Compensated Polymer Optical Fiber Strain Sensors," *IEEE Photo. Tech. Lett.* **24**, 401-403 (2012).

[4] Y. Lin, Y. Zou, Y. Mo, J. Guo and Robert G. "Lindquist E-Beam Patterned Gold Nanodot Arrays on Optical Fiber Tips for Localized Surface Plasmon Resonance Biochemical Sensing," *Sensors* **10**, 9397-9406 (2010).

[5] W. Hong, F. Liang, D. Schaak, M. Loncar, and Q. Quan, "Nanoscale Label-free Bioprobes to Detect Intracellular Proteins in Single Living Cells," *Nature: Scientific Reports* **4**, 6179 (2014).

[6] Z. Tan, X. Hao, Y. Shao, Y. Chen, X. Li, and P. Fan, "Phase modulation and structural effects in a D-shaped all-solid photonic crystal fiber surface plasmon resonance sensor," *Opt. Express* 22, 15049-15063 (2014).

[7] C. Lee, W. Shih, J. Hsu and J. Horng, "Asymmetrical dual tapered fiber Mach-Zehnder interferometer for fiber-optic directional tilt sensor," *Opt. Express* **22**, 24646-24654 (2014).

[8] Q. Chen, C. Jin, Y. Bao, Z. Li, J. Li, C. Lu, L. Yang, and G. Li, "A distributed fiber vibration sensor utilizing dispersion induced walk-off effect in a unidirectional Mach-Zehnder interferometer," *Opt. Express* **22**, 2167-2173 (2014).

[9] T. Zhu, Z. Ou, M. Han, M. Deng, and K. Chiang, "Propylene Carbonate Based Compact Fiber Mach–Zehnder Interferometric Electric Field Sensor," *Journal of Lightwave Technology* **31**, 1566-1572 (2013).

[10] B. Lee, Y. Kim, K. Park, J. Eom, M. Kim, B. Rho and H. Choi, "Interferometric Fiber Optic Sensors," *Sensors* **12**, 2467-2486 (2012).

[11] S. Liu, Y. Wang, C. Liao, G. Wang, Z. Li, Q. Wang, J. Zhou, K. Yang, X. Zhong, J. Zhao, and J. Tang, "High-sensitivity strain sensor based on in-fiber improved Fabry-Perot interferometer," *Opt. Lett.* **39**, 2121-2124 (2014).

[12] Y. Zhang, L. Yuan, X. Lan, A. Kaur, J. Huang, and H. Xiao, "High-temperature fiber-optic Fabry–Perot interferometric pressure sensor fabricated by femtosecond laser," *Opt. Lett.* **38**, 4609-4612 (2013).

[13] D. Yang, H. Tian, and Y. Ji, "Nanoscale photonic crystal sensor arrays on monolithic substrates using side-coupled resonant cavity arrays," *Opt. Express* **19**, Issue 21, 20023-20034 (2011).

[14] Y. Zou, S. Chakravarty, L. Zhu, and R. T. Chen, "The role of group index engineering in series-connected photonic crystal microcavities for high density sensor microarrays," *Appl. Phys. Lett.* **104**, 141103 (2014).

[15] D. Yang, S. Kita, F. Liang, C. Wang, H. Tian, Y. Ji, M. Loncar and Q. Quan, "High sensitivity and high Q-factor nanoslotted parallel quadrabeam photonic crystal cavity for real-time and label-free sensing," *Appl. Phys. Lett.* **105**, 063118, (2014).

[16] D. Yang, H. Tian, and Y. Ji, "Optical Fiber Tips Integrated with High-Q Fano-Resonance Pillar-Array

Photonic-Crystals for High Sensitive Remote Sensing," *2015 Asia Communications and Photonics Conference*, **ACPA-AS4I.5**, Hong Kong, (2015).

[17] S. Chakravarty, W. Lai, Y. Zou, H. Drabkin, R. Gemmill, G. Simon, S. Chin, R. T. Chen, "Multiplexed specific label-free detection of NCI-H358 lung cancer cell line lysates with silicon based photonic crystal microcavity biosensors," *Biosensors and Bioelectronics* **43**, 50-55, (2013).

[18] B. Park, J. Provine, I. Jung, Roger T. Howe, and O. Solgaard, "Photonic Crystal Fiber Tip Sensor for High-Temperature Measurement," *Sensors Journal, IEEE* **11**, 2643-2648 (2011).

[19] O. Kilic, M. Digonnet, G. Kino and O. Solgaard, "External Fiber Fabry-Perot Acoustic Sensor Based on Photonic Crystal Mirror," *Meas. Sci. Technol.* **18**, 3049-3054 (2007).

[20] G. Shambat, S. Kothapalli, A. Khurana, J. Provine, T. Sarmiento, K. Cheng, Z. Cheng, J. Harris, H. Daldrup-Link, S. Gambhir and J. Vuckovic, "A photonic crystal cavity-optical fiber tip nanoparticle sensor for biomedical applications," *Appl. Phys. Lett.* **100**, 213702 (2012).

[21] W. Suh and S. Fan, "All-pass transmission or flattop reflection filters using a single photonic crystal slab," *Appl. Phys. Lett.* **84**, 4905-4907 (2004).

[22] S. Fan and J. D. Joannopoulos, "Analysis of guided resonances in photonic crystal slabs," *Phys. Rev. B* **65**, 235112 (2002).

[23] Y. Shuai, D. Zhao, Z. Tian, J. Seo, D. V. Plant, Z. Ma, S. Fan, and W. Zhou, "Double-layer Fano resonance photonic crystal filters," *Opt. Express* **21**: 24582-24589 (2013).

[24] Y. Kanamori, T. Kitani, and K. Hane, "Control of guided resonance in a photonic crystal slab using microelectromechanical actuators," *Appl. Phys. Lett.* **90**, 031911 (2007).

[25] T. Sar, J. Hagemeier, W. Pfaff, E. Heeres, S. Thon, H. Kim, P. Petroff, O. Tjerk, D. Bouwmeester, and R. Hanson, "Effect of a nanoparticle on the optical properties of a photonic crystal cavity: theory and experiment," *J. Opt. Soc. Am. B* **29**, 698-703 (2012).